Chapter 1

Design of Acridine-N Peptide Conjugates with Enhanced Binding Affinity and Specificity to RNA Targets

Abstract

Arginine-rich peptides and small-molecule intercalating agents provide mechanistically distinct molecular tools for RNA recognition. Here, we have worked to combine these distinct binding modules in an effort to create conjugate ligands with enhanced affinity and specificity using the bacteriophage λ N peptide/boxB RNA interaction as a model system. To do this, we designed and synthesized a series of peptide-acridine conjugates using portions of the N RNA-binding domain (11 and 22 residue peptide segments). We then compared the binding affinities, specificities, salt dependences, and structural properties of the RNA-peptide and RNA-peptide-conjugate complexes using steady-state fluorescence, CD spectroscopy, NMR, and native gel mobility shift assays (GMSA). These analyses revealed that the full-length peptide-acridine conjugate had substantially improved RNA-binding affinity (~80-fold; K_d ~ 20 pM) and specificity (~25-fold) relative to the peptide alone. This binding enhancement was unique to only full length conjugates tested, implying that the structural context of acridine presentation was critical. In line with this view, the specificity enhancement we observe results because binding of the best conjugate to a noncognate P22 RNA hairpin showed only a modest (3-fold) binding enhancement. Our work supports the idea that peptide- and intercalation-based binding can be combined to create a new class of high-affinity, high-specificity RNA-binding ligands.

Introduction

The design of proteins with the capacity to recognize nucleotide sequences with high affinity and specificity has been pursued extensively. The information gained from designing DNA binders include utilizing zinc finger proteins to target sites in the major groove[1-3] and polyamides to target sites in the minor groove.[4-6] The ability of RNA molecules to fold into complex and unique three dimensional shapes and their important roles in many biological processes have generated great interest in designing sequence or structure-specific RNA-binding molecules. Recent successes of sequence-specific RNA binding molecules, the expansion of structural databases for RNA and RNA/protein complexes, together with the development of new synthetic tools, have provided new opportunities for the design of peptide or small molecule RNA binders. One approach to enhance RNA binding is to combine different binding modes using potential interaction sites that coexist in a given RNA molecule. In principle, if two binding sites are in close proximity, a dimeric derivative ligand can bind simultaneously to the two sites, resulting in binding affinity greater than either module.[7,8] This strategy was also demonstrated in our efforts to select peptide-drug conjugates as novel inhibitors of the penicillin binding protein.[9] In vitro selection of peptide-drug conjugates resulted in a penicillin-peptide conjugate that at least 100-fold higher activity than the parent penicillin itself. In this chapter, we discuss the recent successful application of these principles to create novel RNA-binding peptides, with particular emphasis on the advances achieved using intercalating agent acridine.

Recent studies have shown that the tethering of multiple binding modules can enhance RNA-binding affinity and specificity. In particular, acridine derivatives have proved very useful as intercalating modules. In a recent report, a Tat-TAR binding inhibitor consisting of a substituted acridine and a polyamine moiety was demonstrated to inhibit Tat function.[10] Their modular design principle of Tat function impairment was based on the ability of the aromatic moiety of acridine for stacking, and a polycationic anchor for contacts with the TAR RNA phosphate backbone. The two modules are linked by an aliphatic linker. Aside from the compound stacking between two bases, direct hydrogen-bond contacts with a GC base pair were also involved.

In another study, a series of cationic small molecules were synthesized and their binding abilities to defined RNA duplexes with and without bulged bases were investigated.[11] Complex stabilization and selectivity for an RNA duplex containing a single bulged base over a normal RNA duplex have been obtained with a ligand consisting of a chloroacridine moiety covalently attached to 2,6-diaminopurine through an aminoalkyl linker. It is believed that the chloroacridine moiety intercalates into the RNA duplex and the 2,6-diaminopurine interacts with the bulged base.

Another example of this type of binding enhancement is illustrated by a neomycin-acridine conjugate, synthesized by covalently linking neomycin B to 9-aminoacridine via a short spacer, as a potent inhibitor of Rev-RRE binding.[12] Its affinity to the RRE is about 50-fold higher than that of the parent neomycin B and approaches that of the Rev

peptide. These results demonstrate that the combination of different binding modes (e.g., ionic and intercalation) within one ligand is a powerful approach for enhancing the RNA affinity of synthetic binders.

Acridine conjugation has also been used in designing functional molecules. For example, attachment of an acridine moiety to a catalytic tripeptide produced an RNase mimic,[13] and attachment to a nucleic base-linker construct endowed with abasic site recognition generated DNA cleavage function at apurinic sites.[14] Acridine has also been used in conjunction with an oligonucleotide to facilitate site-selective RNA hydrolysis.[15] In this case, acridine was hypothesized to push the bulged base out of the helix and present a scission site.

We reasoned that the same principles may also apply to the N peptide/boxB RNA complex system. Bacteriophage N proteins play an essential role in transcriptional antitermination, which are critical for phage development.[16] The inhibition of transcription termination at intrinsic and Rho-dependent terminators by N protein depends on recognition of a *cis*-acting RNA-element called Nut (N utilization) on the nascent phage transcript. Together with four *Escherichia coli* host factors (NusA, NusB, NusG, and ribosomal protein S10), they form a ribonucleoprotein complex that converts the RNA polymerase into a termination-resistant form. [16,17]

The Nut site consists of a 5'-single-stranded RNA element (boxA) and a 3' hairpin (boxB).[18,19] The boxB from lambda phage is a 15-mer RNA stem-loop hairpin

containing a purine-rich pentaloop (Figure 1). The RNA-binding domain of N protein consists of an arginine-rich motif located at the NH_2-terminus.[20] The 22-residue short peptide recognizes the cognate boxB RNA with similar specificity and affinity as the intact N protein.[21] Upon complex formation, four of the pentaloop nucleotides adopt a canonical GNRA tetraloop fold[22] with the fourth adenine extruded; [23,24] the peptide forms a bent α helix and binds tightly to the major groove of the RNA. [23-25]

The RNA–protein interface of the N_{22}/boxB complex is dominated by electrostatic interactions and hydrophobic contacts.[23] The five arginines and two lysines of N_{22} create a positively charged surface on one face of the α-helix that interacts with the negatively charged phosphodiester backbone of the boxB RNA. Hydrophobic interactions are also important for boxB recognition. Ala-3 and Trp-18 are involved in crucial hydrophobic interactions. In addition, the roles of arginine and lysine residues are not restricted to ionic interactions, and some of the aliphatic portions of these side chains also contact the RNA bases or sugars.

The N/boxB complex is an ideal system for testing binding enhancement by introducing a new binding mode, e.g., intercalation. In this chapter, we report our efforts using acridine-peptide conjugates to enhance N peptide binding affinity against boxB RNA targets and demonstrate the recent successful application of these principles to create novel RNA-binding peptides, with particular emphasis on the advances achieved using intercalating agent acridine.

Materials and Methods

*Synthesis of peptides and acridine-peptide conjugates***.**

Crude peptides with or without linkers were constructed by automated solid phase peptide synthesis using Fmoc protected monomers (ABI) on an Applied Biosystems 432A peptide synthesizer. A series of full length λ N_{22} and truncated λ N_{11} acridine-peptide conjugates were manually synthesized on the resin using the chemistry outlined in Scheme 1. Two types of flexible linkers, a Gly-Gly linker **1** and an ethylene glycol linker **2**, were used. Crude peptides and crude acridine-peptides conjugates were deprotected and cleaved from the resin and purified by reverse-phase HPLC on a C18 column. The purity of the products was checked by analytical HPLC and their identity confirmed by MALDI–TOF mass spectrometry. Concentrations of peptide stocks were determined by UV absorption at 280 nm for free peptides containing either tryptophan or tyrosine, or at 412/434 nm for acridine-peptide conjugates using extinction coefficients (ε=$1.32\times10^4 cm^{-1}M^{-1}$ at 412 nm, and $1.12\times10^4 cm^{-1}M^{-1}$ at 434 nm) determined for a water soluble acridine derivative 3-acridin-9-ylamino-propanol synthesized from 9-chloroacridine and 3-amino-1-propanol as described. [12]

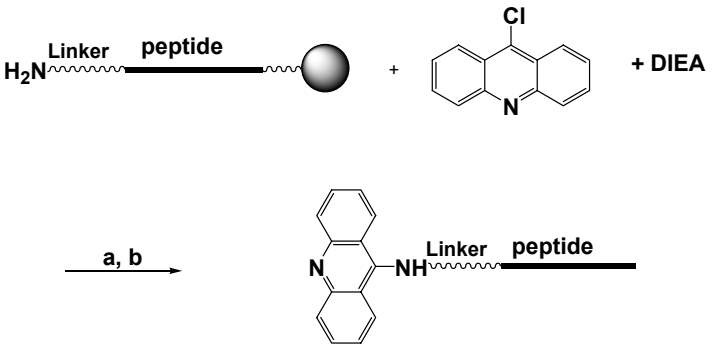

a. phenol, 100^{o}C, 1 h **b. TFA, thioanisole, 1,2-ethanedithiol, 2 h**

Linker = GG or -$CH_2CH_2OCH_2CH_2OCH_2CO$-

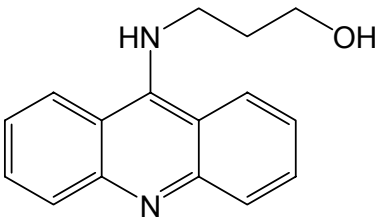

3-acridin-9-ylamino-propanol

λmax (nm)	ε ($cm^{-1}M^{-1}$)
220	$2.84x10^4$
266	$6.99x10^4$
412	$1.32x10^4$
434	$1.12x10^4$

Scheme 1. Synthesis and quantification of acridine-peptide conjugates.

Synthesis of 2AP-labeled RNA oligomers.

Crude RNA oligomers with fluorescent 2- aminopurine (2AP) label substituted for adenine at the 2nd, 3rd, and 4th base positions of the pentaloop (denoted 2AP-2, 2AP-3, and 2AP-4, respectively) were constructed by automated synthesis using 2-aminopurine-TOM-CEphosphoramidite (Glen Research, Sterling, VA). Oligomers were deprotected and purified by 20% urea-PAGE. Purified oligomers were desalted on NAP-25 column and quantified by UV absorption at 260 nm.

Steady-State Fluorescence Measurements.

Steady-state fluorescence measurements were made on a Shimadzu RF-5301PC Spectrofluorophotometer as described. [21,26] Aliquots of concentrated stocks of free peptide or acridine-peptide conjugates were added stepwise to a stirred solution of 2AP-containing RNA maintained at various temperatures in a series of buffer conditions. Fluorescence signal of 2AP was monitored at 370 nm with excitation at 310 nm. Dissociation constants (K_d) were analyzed using the computer program Dynafit. [27]

Band Shift Analysis.

Free *boxB* RNA or complexes of peptide-RNA were preformed in NMR buffer (50 mM NaCl, 10 mM Phosphate, 0.5 mM EDTA, pH 6), and diluted by TBE buffer, before loading to 20% non-denaturing PAGE gel maintained at 10-15 °C. Free RNA and complex bands were visualized by UV shadowing.

One Dimensional NMR Spectroscopy.

Unlabeled 15mer boxB RNA 5'GCCCUGAAAAAGGGC3' (bases in the loop are underlined) was synthesized by in vitro transcription using T7 RNA polymerase.[28] The RNA was purified by 20% urea-PAGE and desalted on a NAP25 column. Purified RNA oligomer was resuspended in NMR buffer (50 mM NaCl, 10 mM Phosphate, 0.5 mM EDTA, pH 6, 90:10 H2O/D2O). Spectra were collected on a Varian INOVA 600 MHz NMR spectrometer at 25 °C. Spectrum of free boxB RNA was collected first; titration of concentrated peptide or acridine peptide conjugate into the boxB RNA was monitored by inspecting the imino proton region of RNA.

CD Spectroscopy.

Spectra were taken on an Aviv 62 DS CD spectrometer at 20°C. The samples contained 5 μM RNA and 6 μM peptide in 10 mM potassium phosphate buffer (pH 7.9). The spectra of the bound peptides were determined by subtracting the spectra for free RNA and excess free peptide from that of the complex.

Results

We envisioned that in the acridine peptide conjugate–RNA complex, the high affinity λ N peptide would bind to the major groove of the boxB RNA with the same structure as in the wild-type complex. [23,24] This would deliver the acridine moiety proximal to the bottom part of the RNA stem (Figure 1) where it can either intercalate into the stem or simply associate with the RNA extrahelically.

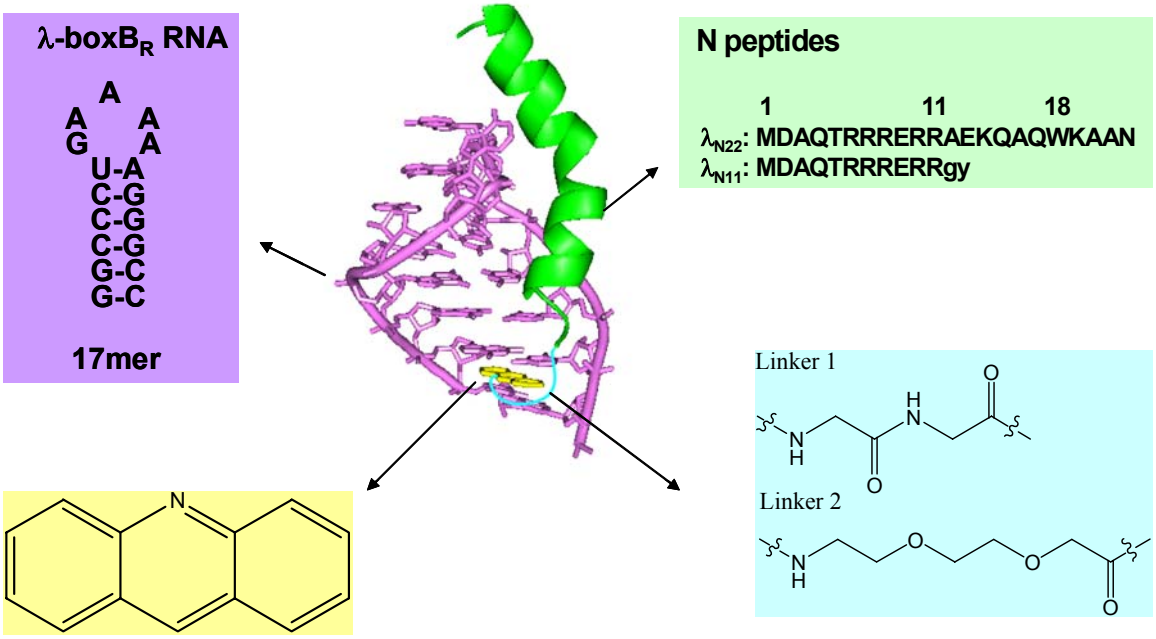

Figure 1. Design of acridine-peptide conjugate binding to boxB RNA**. A**. Sequences and secondary stem-loop structures of boxB RNA from λ bacteriophages used in this study. **B**. Sequences of λ N_{22} full length and truncated λ N_{11} peptides. The 11-mer was tagged with gy for quantification purposes. **C.** Structure of acridine. **D**. Structure of linkers.

K_d values.

Dissociation constants (K_d) were determined by monitoring the change in fluorescence of 2-aminopurine (2AP) incorporated at variable positions within the loops of the RNA hairpins. This base was found to be extremely useful as a probe of nucleic acid structure and dynamics,[29] and RNA-peptide interactions.[26] The fluorescence intensity of 2AP is very sensitive to local environment, decreasing when stacked and increasing when solvent exposed.[30] In most cases, peptide binding can be detected by either a fluorescence increase or decrease of more than 20% from the starting value .[21,31]

Table 1. Dissociation constants (K_d) for peptides and acridine-peptide conjugates against boxB_R RNA[a]

	λ boxB_R RNA targets (17mers)		
	λ-2AP-2	λ-2AP-3	λ-2AP-4
	A A A G A U A C G C G C G G C g c	A A A G A U A C G C G C G G C g c	A A A G A U A C G C G C G G C g c
Peptide	K_d (nM)	K_d (nM)	K_d (nM)
λ_{N11}	1126	1480	1000
Acr-Link1-λ_{N11}	3945	2304	3504
Acr-Link2-λ_{N11}	3082	2200	3245
λ_{N22}	1.9	1.0	1.2
Acr-Link1-λ_{N22}	2.7	1.3	2.0
Acr-Link2-λ_{N22}	0.025[b]	0.019[b]	0.015[b]

[a] Binding constants were determined for standard condition: 20 ˚C; 50 mM KOAc, 20 mM Tris.OAc, pH 7.5. Individual isotherms were fit to a one-step reaction with less than 10% error. Hairpin base positions substituted with 2AP are underlined. Acr- refers to acridine moiety.

[b] Extrapolated from high salt measurement to 50 mM K^+ (see Table 2 and Figure 2).

Table 1 shows the K_d values determined at 50 mM K^+/20 mM Tris for acridine-λ N_{11}, and acridine-λ N_{22} peptide conjugates, compared to those of WT peptides, against boxB RNA targets from λ phages. Binding affinities for truncated λ N_{11} peptide-acridine conjugates constructed with either a Gly-Gly linker **1** or an ethylene glycol linker **2** are similar to the WT λ N_{11} peptide. However, the binding affinities are enhanced when the longer and more flexible linker **2** is used on the full length peptide. The enhancement depends on the actual construct and RNA targets and the conjugates have increased binding specificity. For example, an acridine-full length peptide conjugate has 0.015 nM affinity to the 17mer boxB RNA with 2AP-4 labeling when extrapolated from high salt measurement to 50 mM K^+ (Table 2, Figure 2), corresponding to a 80-fold enhancement over the wild full length peptide (1.2 nM). The longer and more flexible linker **2** seems to provide affinity enhancement. Full length acridine peptide conjugates constructed with the shorter and more rigid linker **1** exhibited no binding enhancement, therefore further investigations were focused on the linker **2**.

Salt dependence of binding.

Generally protein-nucleic acid interactions become weaker as the salt concentration is increased due to the electrostatic nature of binding. This principle also extends to our system. Since N peptide is arginine-rich, the electrostatic interactions between positively charged peptide side chains and negatively charged RNA phosphate backbone are critical for binding.[23] These electrostatic interactions are mitigated by increasing concentration of salt. Within a range of cation concentrations, plots of log (K_d) vs. log [M^+] give a linear relationship. The slope of these plots corresponds to the number of counterions that are released upon peptide binding. In general, the slope is related to the net charge of the peptide and ranges from 2.5 to 5 for the N peptide sequences that have been tested.[32] Salt dependence of acridine full length N peptide conjugate–boxB RNA complex was analyzed using the 17mer RNA with 2AP-4 labeling (Table 2, Figure 2). Most of the isothermal curves show biphasic transitions with the second transition starting after peptide conjugate reaches 1:1 stoichiometry with the RNA target. The K_d values were fit to the first transition. Indeed, higher salt decreased binding affinity of acridine-peptide conjugate to boxB RNA as observed for the WT peptide. The salt dependence graph showed linear relationship at higher salt and leveled off at low salt (Figure 2) as observed previously.[33,34] The slope has a value of 2.9, slightly higher than the value of 2.4 for wild N peptide, indicating roughly three cations are released upon binding.

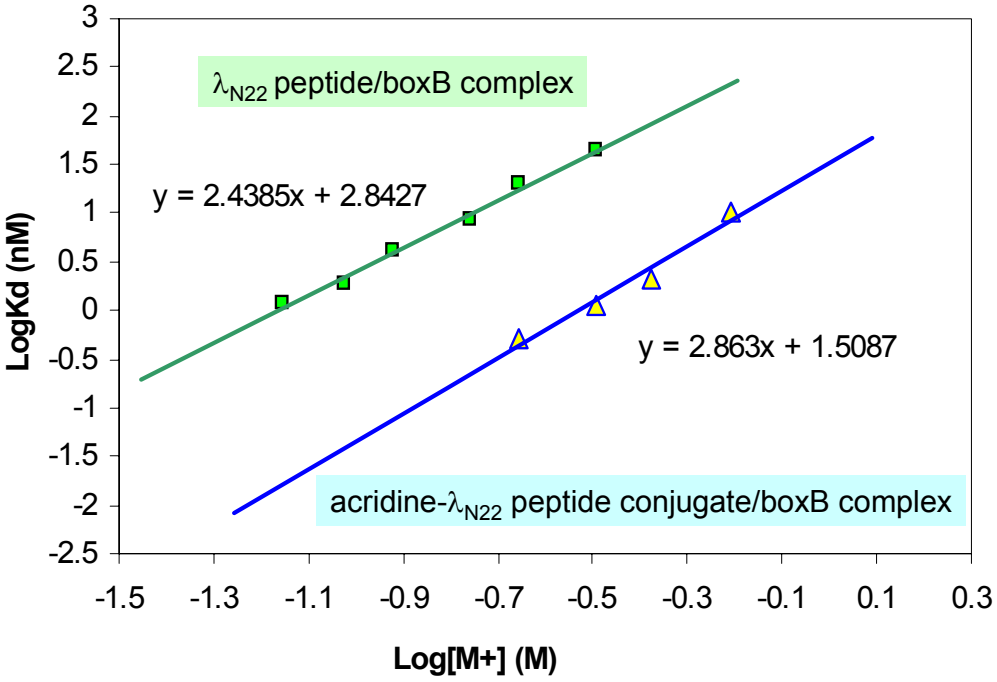

Figure 2. Salt dependence of λ full length peptide (diamond) and acridine-full length peptide conjugate (triangle) binding to 17mer λ boxB RNA (2AP-4). Measurements were made at 20 °C.

The K_d value extrapolated by salt dependence curve to 50 mM K^+, 20mM Tris is 0.015 nM. A roughly 80−fold binding enhancement was observed across a broad range of ionic concentrations. Since the conjugate has slightly higher slope of salt dependence than the free peptide, when extrapolated to lower salt, the enhancement is even higher.

Table 2. Salt dependence*

λ $boxB_R$ RNA target λ-2AP-4(17mer)

A
A A
G A
U A
C G
C G
C G
G C
g c

Peptide	Total monovalent cation concentration (mM) 70	95	120	175	220	320	420	620
	K_d (nM)							
λ_{N22}	1.2	1.9	4.2	8.5	19.8	43.5		
Acr-Link2-λ_{N22}					0.5	1.1	2.1	10

* Total monovalent cation concentration is sum of K^+ and Tris. Binding constants were determined for standard condition: 20 ˚C; 50-600 mM KOAc, 20 mM Tris.OAc, pH 7.5. Individual isotherms were fit to a one-step reaction with less than 10% error. Hairpin base positions substituted with 2AP are underlined. Acr- refers to acridine moiety.

CD Spectra.

The CD spectra collected for both acridine-full length peptide conjugate and free full length peptide binding to boxB RNA (15mer) are shown in Figure 3. Neither the peptide nor the acridine-peptide conjugate shows any appreciable structure in the absence of RNA. The difference spectra of the two complexes indicate that both peptides fold into α helices when bound to the RNA. Although globally similar, the two complexes display some differences in regions indicative of peptide folding (200-225nm) and RNA folding (260-300nm). The acridine conjugate/RNA complex is less α-helical.

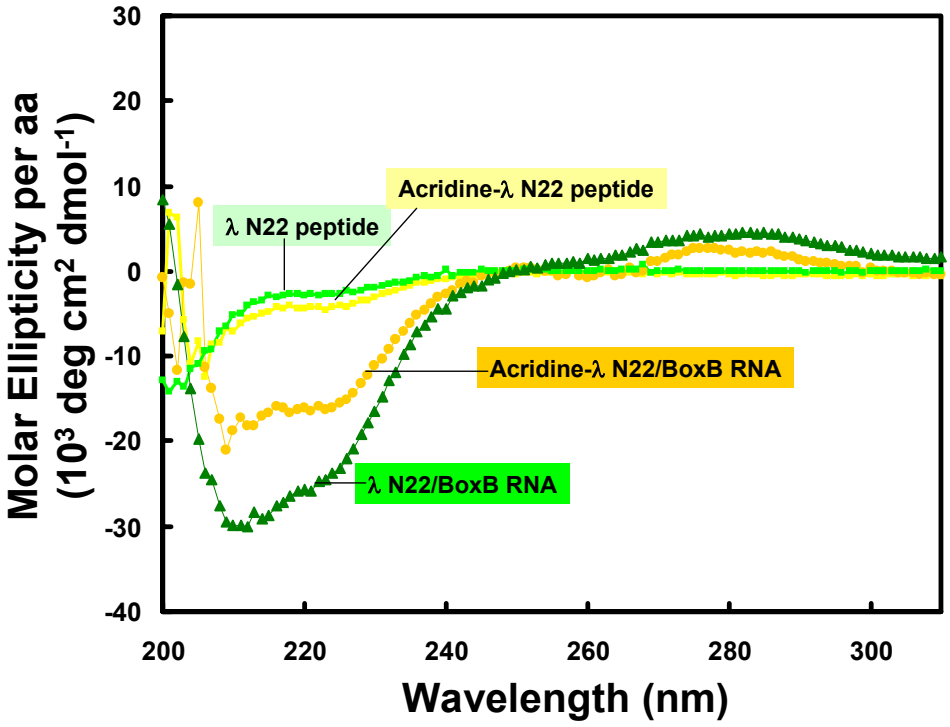

Figure 3. CD spectra of free peptides and peptide/RNA complexes.

NMR Spectroscopy.

NMR experiments can provide useful structural information on the boxB RNA (15mer) and N peptide, especially the structural change upon complexation. In particular, imino protons from RNA base pairs in the stem and Trp18 indole NH proton have unique signals that are easy to monitor. NMR spectra were collected in order to investigate the binding mode between acridine-peptide conjugate and the boxB RNA and compare to that of the free peptide and RNA (Figure 4).

The free 15mer boxB RNA (Figure 4A, a) has 5 base pairs in the stem, the 1D imino proton NMR spectrum showed 3 peaks (13.25 ppm, 12.65 ppm, and 12.55 ppm) corresponding to the imino protons of G12, G13, and G14 from the three middle CG base pairs. The terminal GC pair is not observable due to fraying, and the U imino proton from loop closing UA pair is also missing presumably due to the flexibility of the unstructured pentaloop in the free RNA. Binding by either full length λ N_{22} peptide or truncated amino-terminal λ N_{11} induces similar RNA structural changes, evidenced by shifting of the three CG imino protons to higher field (Figure 4A, b and e). Beside these changes, there were additional imino protons at 13.5 ppm corresponding to U5 of the UA pair, and a broader peak at 10.7 ppm attributable to the G6 imino proton from the sheared GA base pair characteristic of GNRA tetraloop type of folding. This indicates that the loop has been stabilized by peptide binding. In addition, the Trp18 indole NH proton in the full length peptide has a large shift from 10 ppm (Figure 4A, d) in the free peptide to 9.2 ppm in the complex (Figure 4A, e), this is due to the stacking interaction between Trp18 and the RNA loop. [24]

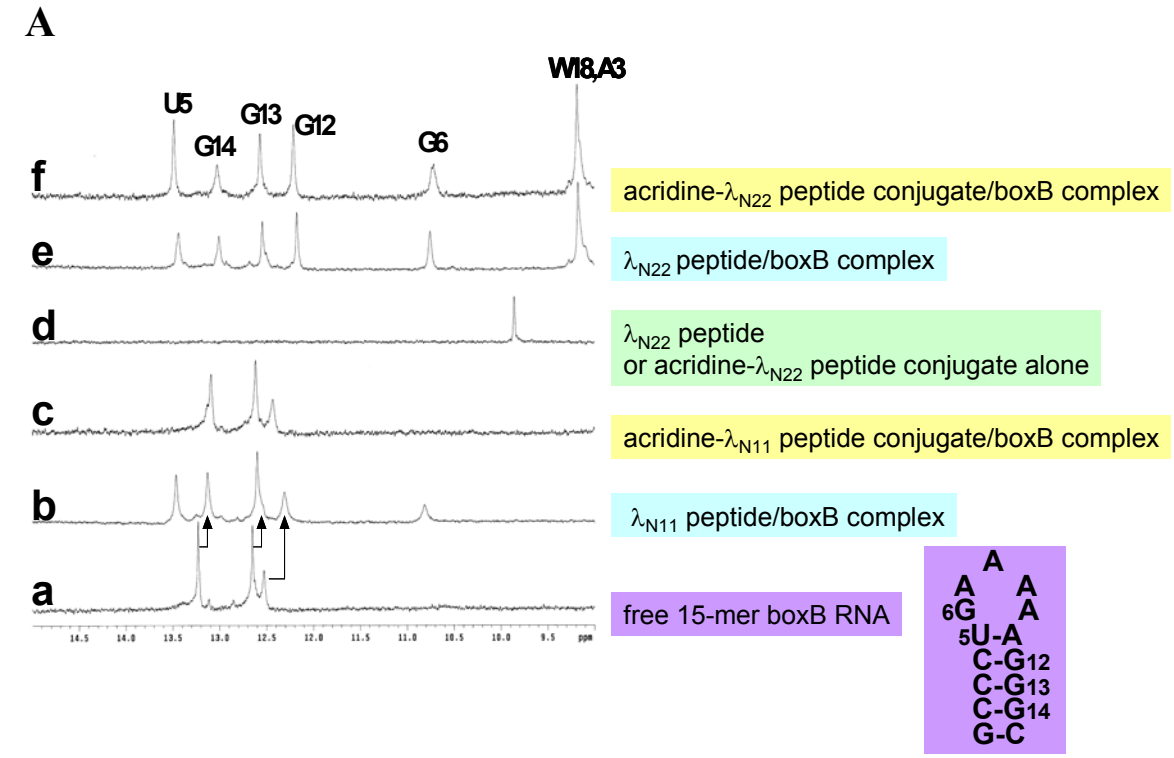

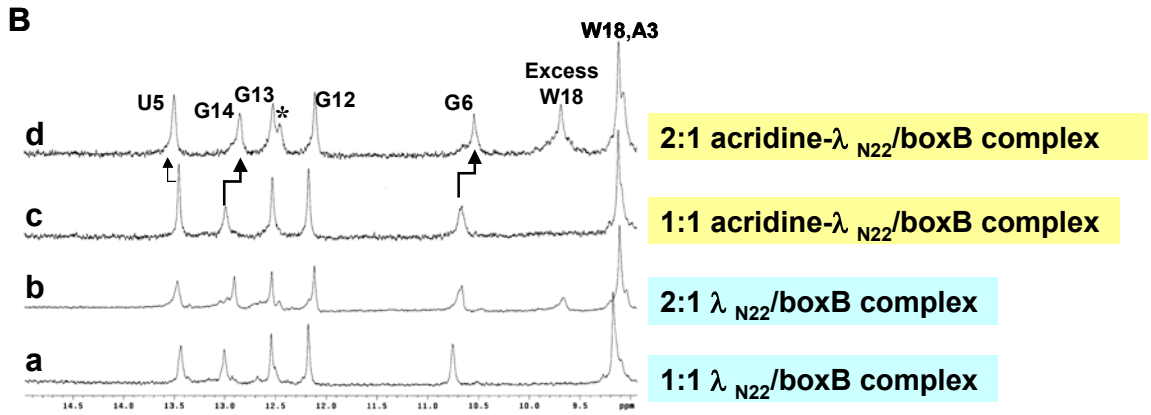

Figure 4. One dimensional NMR spectra for peptide, boxB RNA, and complexes. **A**. Comparison of of λ N_{11} and λ N_{22} peptide/boxB 1:1 ratio complexes. **B**. Comparison of 1:1 peptide/boxB complex and 2:1 peptide/boxB complex. The asterisk indicates the additional peak.

In comparison, the spectrum for acridine-λ N_{11} conjugate complexed to boxB RNA (Figure 4A, c) did not show these characteristic signal changes as observed in λ N_{11} peptide/RNA complex, except for broadening of the original three peaks. This indicates that the acridine-λ N_{11} conjugate does not bind the RNA in the same mode as the λ N_{11} peptide. Since acridine compound 2-acridin-9-ylamino-propanol binds to boxB RNA with about 15 μM affinity, similar to the affinity between λ N_{11} peptide and boxB RNA, it is possible that the two modules compete for the RNA binding site, and acridine moiety can associate with the RNA non-specifically, disrupting the specific complex structure between λ N_{11} peptide and boxB RNA.

The spectrum for 1:1 acridine-full length peptide conjugate/boxB RNA complex (Figure 4A, f) showed very similar imino proton signals for RNA component and characteristic Trp18 indole proton shift as seen in the spectrum for λ N_{22} peptide complex. Within the acridine-full length peptide conjugate, it seems likely that the peptide portion binds the RNA in the same mode as in the WT λ N_{22} peptide complex. This should deliver the acridine moiety to the lower part of boxB RNA stem.

Since acridine-full length peptide conjugate showed biphasic binding to boxB RNA, we further investigated the potential second binding site on boxB RNA for the conjugate. Over titration of the conjugate produced a 2:1 ratio of conjugate:RNA complex. Comparison of the spectra for 1:1 and 2:1 complexes of both WT peptide and acridine-peptide conjugate revealed interesting discrepancies (Figure 4B). For the case of 2:1 acridine-λ N_{22} peptide conjugate/boxB complex, the imino protons for U5 moved further down field, and G6 and G14 moved up field, respectively; furthermore, there is an

additional peak at 12.4 ppm. These features suggest a specific second binding site for the acridine-peptide conjugate.

Band Shift Analysis.

Observations from NMR experiments are consistent with the band shift analysis shown in Figure 5. Because the λ N_{11} peptide binds the boxB RNA specifically, a band shift can be observed (lane 2 of Figure 5A); while there is only smearing in the acridine-λ N_{11} peptide conjugate with boxB RNA (lane 3 of Figure 5A) indicating non-specific interaction, possibly random intercalation of acridine either in the stem or in the loop region which compete with the binding of peptide portion.

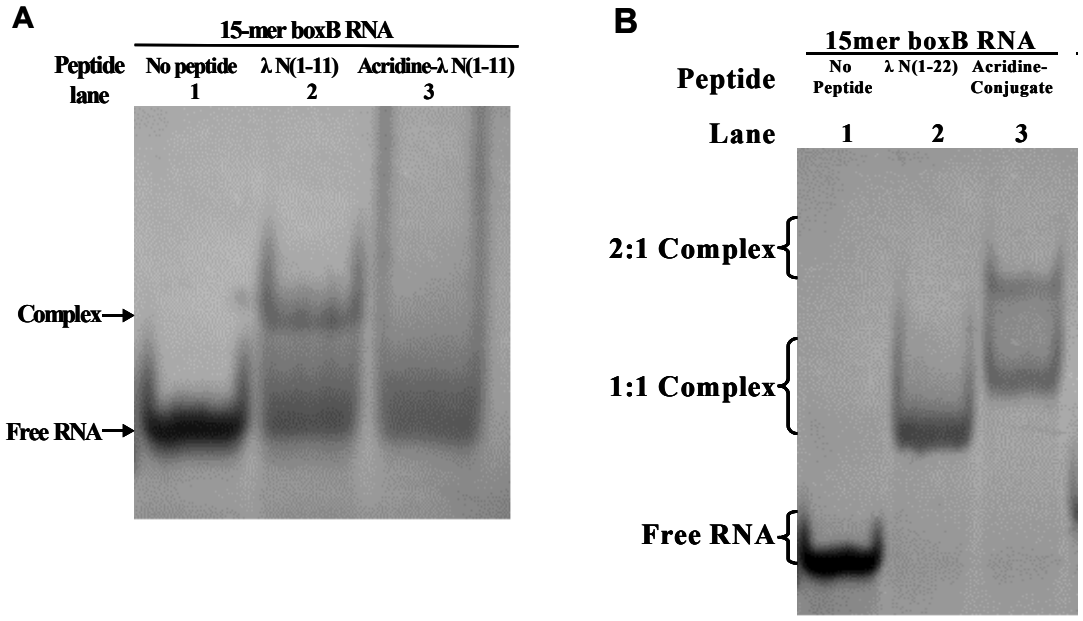

Figure 5. Gel shift analysis of peptide/boxB complexes for WT peptides and acridine-peptide conjugates. **A**. λ N_{11}/RNA and acridine-λ N_{11}/RNA complexes. **B**. λ N_{22}/RNA and acridine-λ N_{22}/RNA complexes.

The acridine full length conjugate, however, not only showed a 1:1 complex to boxB RNA 15-mer (lane 3 of Figure 5B) as in peptide-RNA complex (lane 2 of Figure 5B), but a higher stoichiometric complex as well. These results suggest that there is a second binding site for the acridine-peptide conjugate. This may explain the profile of the fluorescence titration curves, which sometimes show biphasic transitions with the second transition apparently following equimolar titration.

Discussions

To achieve higher RNA binding affinities, the design of a ligand consisting of two moieties connected by a linker is a promising approach. [7,8] Higher binding affinities could result from a favorable entropic factor compared with the binding of the two monomeric counterparts. Sometimes the length and nature of the linker is critical. The molecule can be a dimeric form of a known binder [35] or can consist of two distinct moieties that bind to RNA in different modes, e.g., groove binding and intercalation.[10-12] To apply this idea to the N peptide system, a series of λ N peptide-based peptide-acridine conjugates were designed and synthesized. Their binding affinities to boxB RNAs with stem-loop hairpin structures were determined by steady-state fluorescence measurements.

Since acridine compound 2-acridine-9-ylamino-propanol binds boxB RNA with 15 μM affinity, theoretically, it can provide up to three orders of magnitude enhancement when linked to another binding module. The full enhancement may never be realized in real systems. From comparing salt dependence of binding, acridine-peptide conjugation showed 80-fold binding enhancement over a broad range of salt concentrations. This result is similar to binding enhancement observed for a neo-acridine construct over neomycin B alone binding to RRE RNA.[12] The same construct showed 3-fold tighter binding to a related P22 boxB RNA target. Compared to λ boxB, this RNA has orientation of one base pair in the stem flipped, and a cytidine in the loop instead of

adenine (Figure 6). Both λ_{N22} and $P22_{N21}$ full-length peptides discriminate strongly between their cognate RNA hairpins and other boxB targets.[32] The acridine-peptide conjugates showed enhanced binding specificity between these two similar RNA structures (Table 3). Therefore, the actual enhancement by acridine conjugation depends on the targets involved.

Table 3. Dissociation constants (K_d) for peptides and acridine-peptide conjugates against λ boxB and P22 $boxB_R$ RNA[a]

	$boxB_R$ RNA targets (17mers)	
	λ-2AP-4	P22-2AP-4
	A A A G A U A C G C G C G G C g c	C A A G A U A C G G C C G G C g c
Peptide	K_d (nM)	K_d (nM)
λ_{N22}	1.2	257
Acr-Link2-λ_{N22}	0.015[b]	80

[a] Binding constants were determined for standard condition: 20 ˚C; 50 mM KOAc, 20 mM Tris.OAc, pH 7.5. Individual isotherms were fit to a one-step reaction with less than 10% error. Hairpin base positions substituted with 2AP are underlined. Acr- refers to acridine moiety.

[b] Extrapolated from high salt measurement (Figure 2)

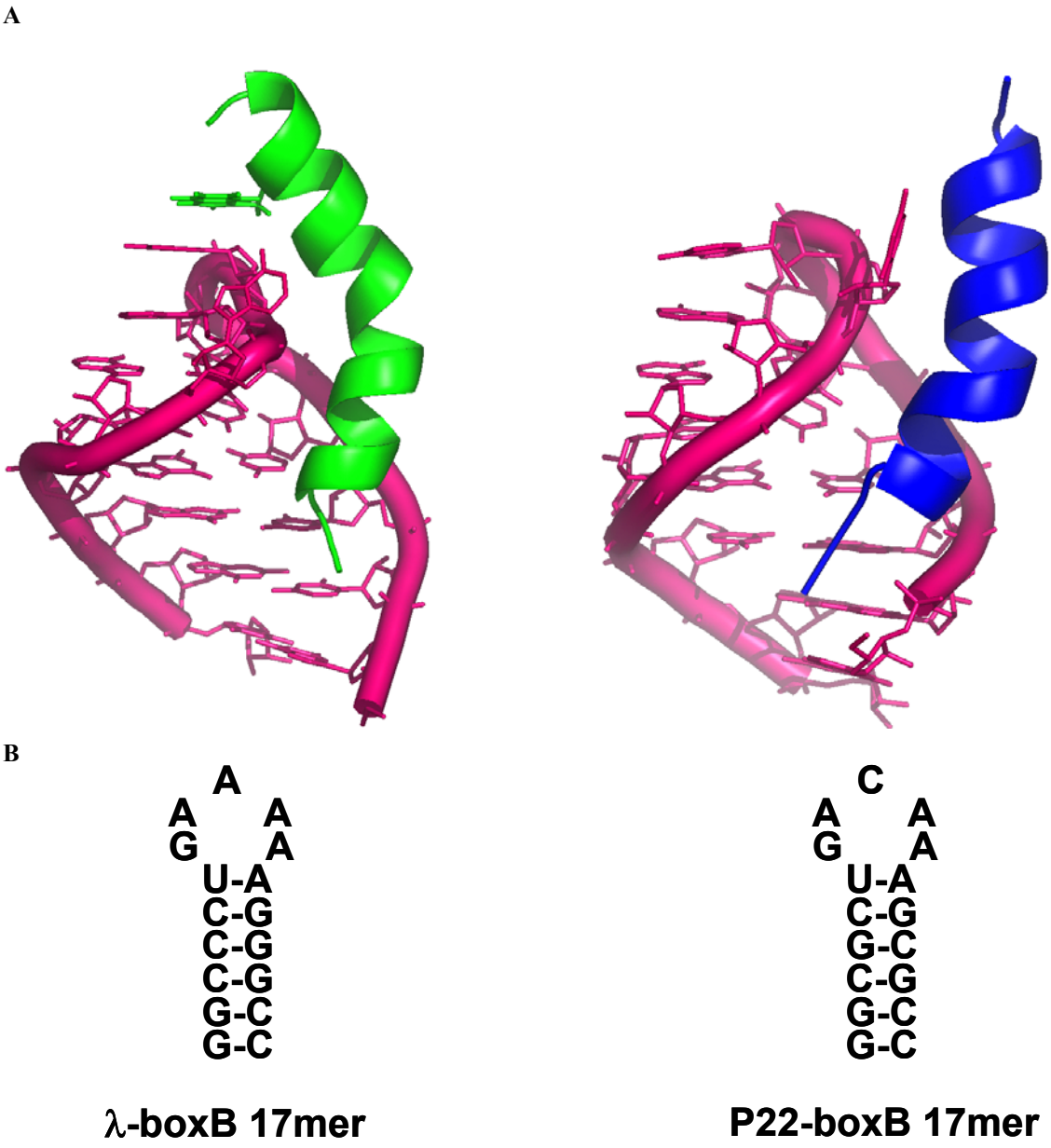

Figure 6. Comparison of λ boxB and P22 boxB RNA. **(A)** Structural models of phage λ and P22 N peptide-boxB hairpin complexes viewed from the major groove. In all complexes the N peptide is shown as a ribbon; **(B)** Schematic representation of λ and P22 boxB hairpin stem-loop structure.

Homologous hydrophobic interactions occur between the boxB hairpin stem and conserved alanine residues within the N peptide amino-terminal module. Distinct hydrophobic interactions appear between the boxB hairpin loops and carboxy-terminal modules of the N peptides. In λ, a tryptophan residue stacks on the boxB loop; in P22, non-polar alanine and isoleucine residues interact with an extruded pyrimidine. In phage λ and P22, the bound pentaloops adopt stable GNRA tetraloop folds by extruding either loop base 4 (4-out) in the λ complex, or loop base 3 (3-out) in the P22 complex.

In contrast, conjugation of acridine to the λ N_{11} peptide did not improve binding. In fact, the conjugate bound about 3-fold weaker than the λ N_{11} peptide alone. The NMR and gel shift data showed that the conjugate does not form a specific complex with boxB RNA (Figure 4A and 5A). Presumably this is due to the fact that the acridine moiety has similar affinity to the boxB RNA compared to the the λ N_{11} peptide, and acridine binding is non-specific. Therefore the acridine moiety competes the binding sites of RNA structure with peptide moiety. This result suggests that when designing a ligand with multiple binding modules, it is important to avoid a non-specific binding module that can compete multiple sites intended for the other modules. A module with higher affinity for one site will help anchor the entire ligand. The specific binding peptide module of the full length acridine-peptide conjugate has much higher affinity for the λboxB RNA, the peptide portion maintains all the native contacts with RNA (Figure 4A), and the acridine moiety can be specifically delivered to the intended site.

Previous structural studies on DNA intercalated with acridine related compounds have consistently shown intercalation site at alternating base steps, particularly at the terminal base steps.[36] This is likely due to the fact that terminal base steps have much greater conformational freedom than internal base steps, which facilitates intercalation. Recent studies on DACA, an antitumor acridine derivatized with variable functional substitutions at position 4, showed that they intercalate into DNA with side chains lying in the major groove.[37-39] However, the crystal structure of an acridine-tetraarginine conjugate with the peptide attached to the position 9 showed intercalation of acridine into the minor groove of central AA/TT base step of a long DNA fragment, leaving the peptide lying in the minor groove.[40]

In these cases, it appeared that specific hydrogen bonding interactions between the lateral chain of acridine and DNA may affect how the acridine moiety intercalates into nucleic acids. Interestingly, a recent study also showed that in peptide-acridine conjugates, the point of attachment on acridine affects the conjugates' affinity for nucleic acid target.[41]

Our acridine-N peptide conjugates feature the peptide portion attaching to the acridine at position 9, similar to the acridine-tetraarginine case. To determine the precise binding mode of acridine in these conjugates is challenging at this time. There may be multiple reasons for this. If the acridine moiety derivatized at position 9 with a peptide

prefers intercalation from minor groove as in the case of acridine-tetraarginine,[40] our construct may preclude intercalation, because full length N peptide binds boxB RNA in the major groove with high affinity. In the case of the acridine-λ N_{11} conjugate, the acridine may be able to intercalate into minor groove, but this intercalation is probably non-site-specific. A second reason is that once the N peptide (especially the full length) binds to boxB RNA peptide induces RNA folding. There are extensive interactions between peptide and RNA stem, an intercalated acridine moiety in the stem may disrupt specific interactions between RNA and peptide. However, the acridine may still be able to intercalate at the terminal base step, but since the imino proton from the terminal base pair is not observable, this possibility has not been confirmed.

Similar to the neo-acridine case[12] where there was a second binding site, our fluorescence, NMR, and gel shift data also suggested a second specific binding site for acridine-N peptide conjugate on boxB RNA. The nature of the second site is not known, but it may be in either the major or minor groove. Changes of the imino proton chemical shifts can be observed throughout the RNA structure (Figure 4B), suggesting that the interactions may be extensive.

Other approaches of enhancing RNA binding affinity may also be available. N peptides bind boxB RNA in an α-helical conformation, but have little helical structure when free in solution.[25] Stabilizing the helical form of such peptides is expected to favor RNA binding by virtue of pre-organization. For example, C^{α}-substituted amino acids has long been recognized as a means of introducing local conformational restriction in

peptides.[42] Another approach to stabilize the α-helical form of peptides is through the incorporation of covalent linkages between constituent amino acid side chains. It was found that substantial helix stabilization was achieved when the linkage was placed between the *i* and *i+4* residue in the peptide backbone by ring closing metathesis.[43-46] Therefore, cyclic helical N peptides, wherein ring closing metathesis is used to incorporate a carbon-carbon tether between appropriate residue side chains, is expected to provide binding enhancement. This approach provides a convenient way to enhance the affinity of known modules and facilitates the discovery of powerful new hybrid ligands with new functionalities.

Conclusion

Designing ligands that consist of multiple modules for binding RNA targets can be a powerful approach to achieve high affinity and specificity. A series of full-length or truncated acridine-peptide conjugates based on the N peptide of bacteriophage λ were designed and synthesized. Their binding affinities to a series of *Box B* RNAs with stem-loop hairpin structures were determined using steady-state fluorescence measurements. Thermodynamic parameters have been characterized for these complexes using salt dependence. An 80-fold binding enhancement of acridine-peptide conjugate with *Box B* RNA was exhibited across a range of salt concentrations. NMR, gel shift, and CD data also indicated the N peptide-acridine conjugate/*Box B* RNA complex formation.

References

1. Klug, A. Zinc finger peptides for the regulation of gene expression. *J Mol Biol* **293**, 215-8 (1999).
2. Segal, D. J. & Barbas, C. F., 3rd. Design of novel sequence-specific DNA-binding proteins. *Curr Opin Chem Biol* **4**, 34-9 (2000).
3. Wolfe, S. A., Nekludova, L. & Pabo, C. O. DNA recognition by Cys2His2 zinc finger proteins. *Annu Rev Biophys Biomol Struct* **29**, 183-212 (2000).
4. White, S., Szewczyk, J. W., Turner, J. M., Baird, E. E. & Dervan, P. B. Recognition of the four Watson-Crick base pairs in the DNA minor groove by synthetic ligands. *Nature* **391**, 468-71 (1998).
5. Dervan, P. B. Molecular recognition of DNA by small molecules. *Bioorg Med Chem* **9**, 2215-35 (2001).
6. Fechter, E. J. & Dervan, P. B. Allosteric inhibition of protein--DNA complexes by polyamide--intercalator conjugates. *J Am Chem Soc* **125**, 8476-85 (2003).
7. Michael, K. & Tor, Y. Designing novel RNA binders. *Chem. Eur. J.* **4**, 2091-2098 (1998).
8. Cheng, A. C., Calabro, V. & Frankel, A. D. Design of RNA-binding proteins and ligands. *Curr Opin Struct Biol* **11**, 478-84 (2001).
9. Li, S. & Roberts, R. W. A novel strategy for in vitro selection of Peptide-drug conjugates. *Chem Biol* **10**, 233-9 (2003).
10. Hamy, F. et al. A new class of HIV-1 Tat antagonist acting through Tat-TAR inhibition. *Biochemistry* **37**, 5086-95 (1998).

11. Wilson, W. D. et al. Bulged-Base nucleic acids as potential targets for antiviral drug action. *New J. Chem.* **18**, 419-23 (1994).

12. Kirk, S. R., Luedtke, N. W. & Tor, Y. Neomycin-acridine conjugate: A potent inhibitor of Rev-RRE binding. *J Am Chem Soc* **122**, 980-981 (2000).

13. Tung, C. H., Wei, Z., Leibowitz, M. J. & Stein, S. Design of peptide-acridine mimics of ribonuclease activity. *Proc Natl Acad Sci U S A* **89**, 7114-8 (1992).

14. Fkyerat, A., Demeunynck, M., Constant, J.-F., Michon, P. & Lhomme, J. A New Class of Artificial Nucleases That Recognize and Cleave Apurinic Sites in DNA with Great Selectivity and Efficiency. *J Am Chem Soc* **115**, 9952-9959 (1993).

15. Kuzuya, A., Mizoguchi, R., Morisawa, F., Machida, K. & Komiyama, M. Metal ion-induced site-selective RNA hydrolysis by use of acridine-bearing oligonucleotide as cofactor. *J Am Chem Soc* **124**, 6887-94 (2002).

16. Greenblatt, J., Nodwell, J. R. & Mason, S. W. Transcriptional antitermination. *Nature* **364**, 401-6 (1993).

17. Das, A. Control of transcription termination by RNA-binding proteins. *Annu Rev Biochem* **62**, 893-930 (1993).

18. Salstrom, J. S. & Szybalski, W. Coliphage lambdanutL-: a unique class of mutants defective in the site of gene N product utilization for antitermination of leftward transcription. *J Mol Biol* **124**, 195-221 (1978).

19. Olson, E. R., Tomich, C. S. & Friedman, D. I. The nusA recognition site. Alteration in its sequence or position relative to upstream translation interferes with the action of the N antitermination function of phage lambda. *J Mol Biol* **180**, 1053-63 (1984).

20. Lazinski, D., Grzadzielska, E. & Das, A. Sequence-specific recognition of RNA hairpins by bacteriophage antiterminators requires a conserved arginine-rich motif. *Cell* **59**, 207-18 (1989).

21. Barrick, J. E., Takahashi, T. T., Ren, J., Xia, T. & Roberts, R. W. Large libraries reveal diverse solutions to an RNA recognition problem. *Proc Natl Acad Sci U S A* **98**, 12374-8 (2001).

22. Heus, H. A. & Pardi, A. Structural features that give rise to the unusual stability of RNA hairpins containing GNRA loops. *Science* **253**, 191-4 (1991).

23. Legault, P., Li, J., Mogridge, J., Kay, L. E. & Greenblatt, J. NMR structure of the bacteriophage lambda N peptide/boxB RNA complex: recognition of a GNRA fold by an arginine-rich motif. *Cell* **93**, 289-99 (1998).

24. Scharpf, M. et al. Antitermination in bacteriophage lambda. The structure of the N36 peptide-boxB RNA complex. *Eur J Biochem* **267**, 2397-408 (2000).

25. Su, L. et al. RNA recognition by a bent alpha-helix regulates transcriptional antitermination in phage lambda. *Biochemistry* **36**, 12722-32 (1997).

26. Lacourciere, K. A., Stivers, J. T. & Marino, J. P. Mechanism of neomycin and Rev peptide binding to the Rev responsive element of HIV-1 as determined by fluorescence and NMR spectroscopy. *Biochemistry* **39**, 5630-41 (2000).

27. Kuzmic, P. Program DYNAFIT for the analysis of enzyme kinetic data: application to HIV proteinase. *Anal Biochem* **237**, 260-73 (1996).

28. Milligan, J. F., Groebe, D. R., Witherell, G. W. & Uhlenbeck, O. C. Oligoribonucleotide synthesis using T7 RNA polymerase and synthetic DNA templates. *Nucleic Acids Res* **15**, 8783-98 (1987).

29. Menger, M., Eckstein, F. & Porschke, D. Dynamics of the RNA hairpin GNRA tetraloop. *Biochemistry* **39**, 4500-7 (2000).

30. Rachofsky, E. L., Osman, R. & Ross, J. B. Probing structure and dynamics of DNA with 2-aminopurine: effects of local environment on fluorescence. *Biochemistry* **40**, 946-56 (2001).

31. Austin, R. J., Xia, T., Ren, J., Takahashi, T. T. & Roberts, R. W. Designed Arginine-Rich RNA-Binding Peptides with Picomolar Affinity. *J Am Chem Soc* **124**, 10966-7 (2002).

32. Austin, R. J., Xia, T., Ren, J., Takahashi, T. T. & Roberts, R. W. Differential Modes of Recognition in N Peptide-BoxB Complexes. *Biochemistry* **42**, 14957-67 (2003).

33. Record, M. T., Jr., Lohman, M. L. & De Haseth, P. Ion effects on ligand-nucleic acid interactions. *J Mol Biol* **107**, 145-58 (1976).

34. Record, M. T., Jr., Ha, J. H. & Fisher, M. A. Analysis of equilibrium and kinetic measurements to determine thermodynamic origins of stability and specificity and mechanism of formation of site-specific complexes between proteins and helical DNA. *Methods Enzymol* **208**, 291-343 (1991).

35. Campisi, D. M., Calabro, V. & Frankel, A. D. Structure-based design of a dimeric RNA-peptide complex. *Embo J* **20**, 178-86 (2001).

36. Williams, L. D., Egli, M., Gao, Q. & Rich, A. (eds.) *Nucleic Acids* (Adenine Press, Schenectady, NY, 1992).

37. Todd, A. K. et al. Major groove binding and 'DNA-induced' fit in the intercalation of a derivative of the mixed topoisomerase I/II poison N-(2-

(dimethylamino)ethyl)acridine-4-carboxamide (DACA) into DNA: X-ray structure complexed to d(CG(5-BrU)ACG)2 at 1.3-A resolution. *J Med Chem* **42**, 536-40 (1999).

38. Adams, A., Guss, J. M., Denny, W. A. & Wakelin, L. P. Crystal structure of 9-amino-N-[2-(4-morpholinyl)ethyl]-4-acridinecarboxamide bound to d(CGTACG)2: implications for structure-activity relationships of acridinecarboxamide topoisomerase poisons. *Nucleic Acids Res* **30**, 719-25 (2002).

39. Adams, A., Guss, J. M., Collyer, C. A., Denny, W. A. & Wakelin, L. P. Crystal structure of the topoisomerase II poison 9-amino-[N-(2-dimethylamino)ethyl]acridine-4-carboxamide bound to the DNA hexanucleotide d(CGTACG)2. *Biochemistry* **38**, 9221-33 (1999).

40. Malinina, L., Soler-Lopez, M., Aymami, J. & Subirana, J. A. Intercalation of an Acridine-Peptide Drug in an AA/TT Base Step in the Crystal Structure of [d(CGCGAATTCGCG)](2) with Six Duplexes and Seven Mg(2+) Ions in the Asymmetric Unit. *Biochemistry* **41**, 9341-9348 (2002).

41. Carlson, C. B. & Beal, P. A. Point of attachment and sequence of immobilized Peptide-acridine conjugates control affinity for nucleic acids. *J Am Chem Soc* **124**, 8510-1 (2002).

42. Liff, M. I., Kopple, K. D., Tian, Z. & Roeske, R. W. Effects of C alpha-methyl substitution on the conformation of linear GnRH antagonist analogs. *Int J Pept Protein Res* **43**, 471-6 (1994).

43. Miller, S. J. & Grubbs, R. H. Synthesis of Conformationally Restricted Amino-Acids and Peptides Employing Olefin Metathesis. *J Am Chem Soc* **117**, 5855-5856 (1995).

44. Lynn, D. M., Mohr, B. & Grubbs, R. H. Living ring-opening metathesis polymerization in water. *J Am Chem Soc* **120**, 1627-1628 (1998).

45. Blackwell, H. E. & Grubbs, R. H. Highly efficient synthesis of covalently cross-linked peptide helices by ring-closing metathesis. *Ange Chem-Int Ed* **37**, 3281-3284 (1998).

46. Schafmeister, C. E., Po, J. & Verdine, G. L. An all-hydrocarbon cross-linking system for enhancing the helicity and metabolic stability of peptides. *J Am Chem Soc* **122**, 5891-5892 (2000).